Microstructural and mechanical analysis of 316L SS/ β-TCP composites produced though the powder metallurgy route

http://dx.doi.org/10.1590/0370-44672017710175

Mônica Huguenin de Araújo Faria[1]
Alexandre Nogueira Ottoboni Dias[2]
Leonardo Albergaria Oliveira[3]
http://orcid.org/0000-0001-8810-4987
Claudiney de Sales Pereira Mendonça[4]
Bruna Horta Bastos Kuffner[5]
http://orcid.org/0000-0003-3306-5102
Daniela Sachs[6]
Gilbert Silva[7]

[1]Doutora em Físico-Química e Pesquisadora, Universidade Estadual de Campinas – UNICAMP, Campinas – São Paulo – Brasil.
monica.ifsp@hotmail.com

[2]Doutor em Materiais para Engenharia e Professor-Substituto, Universidade Federal de Itajubá – UNIFEI, Itajubá – Minas Gerais – Brasil.
aottoboni@yahoo.com.br

[3]Doutor em Engenharia Mecânica, Universidade Federal de Itajubá – UNIFEI, Itajubá – Minas Gerais – Brasil.
leonardoeng1@gmail.com, leonardoeng1@yahoo.com.br

[4]Doutor em Materiais para Engenharia, Universidade Federal de Itajubá - UNIFEI, Departamento de Física e Química, Itajubá – Minas Gerais – Brasil.
sales.claudiney21@gmail.com

[5]Doutoranda em Materiais para Engenharia, Universidade Federal de Itajubá – UNIFEI, Itajubá – Minas Gerais – Brasil.
brunakuffner@hotmail.com

[6]Doutora em Ciências e Professora-Adjunta, Universidade Federal de Itajubá – UNIFEI, Itajubá – Minas Gerais – Brasil.
danisachs@unifei.edu.br

[7]Doutor em Engenharia Biomédica e Professor-Adjunto, Universidade Federal de Itajubá – UNIFEI, Itajubá – Minas Gerais – Brasil.
gilbert@unifei.edu.br

Abstract

The 316L stainless steel (316L SS) is one of the most used metallic materials for implants, due to its high mechanical properties and low cost. However, it is bioinert. One possibility to improve its biocompatibility is the production of a composite with β-tricalcium phosphate (β- TCP) addition. This study investigated the mechanical behavior of 316L SS/β-TCP composites through powder metallurgy. For this, used were 3 compositions, with 0 %, 5 % and 20 % of β-TCP. The compositions with 5% and 20% were milled during 10 hours with a mass/sphere ratio of 1:10 and 350 rpm. All compositions were uniaxially pressed with 619 MPa and sintered during 1 hour at 1100°C. The microstructural and mechanical evaluations were performed through scanning electron microscopy, density and compressive strength. The results indicated that, by increasing the percentage of β-TCP in the compositions, the mechanical resistance decreases, as a consequence of its low load support.

Keywords: beta tricalcium phosphate, 316L stainless steel, composites, powder metallurgy.

1. Introduction

In general, the primary destination of metallic biomaterials is in the orthopedic field for the manufacture of prostheses; implants to replace bone tissue and fastening devices (the fastening devices are used to stabilize fractured bones while bone regeneration occurs). The main reason that leads medical companies to use metallic biomaterials to produce orthopedic devices is due to their ability to withstand significant loads, their high fatigue resistance and ability to suffer plastic deformation before failure, properties that are not possible to achieve in pure ceramic or polymeric biomaterials (Lin *et al*., 2016; Lai *et al*., 2018).

An important parameter used to decide the correct material for a specific destination, in terms of mechanical applications, is the Young's modulus. If the Young's modulus of the material used to manufacture an implant is much higher than the bone, the load support is not considered ideal. Consequently, this can result in a mechanical isolation of the material, and the equilibrium of tension observed to induce the bone remodeling is hampered, occurring then the loosening of the prosthesis (Rao *et al*., 2017; Bobbert *et al*., 2017, Kuffner *et al*., 2015).

Some of the metals more commonly used to manufacture implants include the 316L stainless steel, the titanium-aluminum-vanadium (Ti 6Al 4V) and Co-Cr alloys. The 316L SS is a material that presents lower cost than the titanium-aluminum-vanadium and Co-Cr alloys. Also, it is easily accessible, which makes it a suitable material in the medical industry, especially for applications such as orthopedic implants. However, the 316L SS is bioinert, which complicates its integration with the bone tissue, causing the reduction of the durability of the implant. A strategy widely used is the 316L SS coating applied with other materials, such as the calcium phosphate ceramics (CPCs) (Sing *et al*., 2016; Jenko *et al*., 2017; Kaita *et al*., 2018).

The calcium phosphate ceramics (CPCs) are a class of biocompatible and bioactive materials widely used for bone tissue repair. The CPCs have ideal surface properties for the adhesion and proliferation of osteoblasts, stimulating the formation of new bone, being thus considered osteoconductive and osteoinductive. The osteoinductive capacity of the CPCs in vivo is associated with the solubility and capacity of reabsorption that they present. The CPC tricalcium phosphate (TCP) occurs in two phases: α and β. However, β-TCP is most commonly used in bone regeneration. Despite the excellent bioactive and biocompatible properties, the CPCs have low fracture resistance and low bearing capacity, which limits their application without a reinforcement. Thus, recent works have sought to increase the load capacity and resistance of the CPCs using other materials, as reinforcement, such as metals or alloys (Ataollahi *et al*., 2015; Torres *et al*., 2016).

In this direction, the main objective of this study was to produce through the powder metallurgy route, a composite with 316L SS and β-TCP, combining the good mechanical properties of the steel and the excellent bioactive characteristic of the ceramic. Studies like Kuffner *et al*. 2017 also studied the microstructural and mechanical behaviour of metal-ceramic composites through powder metallurgy with high energy ball milling, being thus used as a reference in this study.

2. Materials and methods

The β-TCP was purchased from the company Vetec® with an average particle size of 5 μm and density of 3.14 g/cm^3. The 316L stainless steel powder was purchased from the company Lupatech® S/A, with particle size below 20 μm and density of 3.95 g/cm^3 . For the milling process of the composites, used was a high-energy planetary mill Noah-Nuoya® NQM 0.2 L with rotation of 350 rpm, ball to powder mass ratio of 1:10 and milling time of 10 hours.

The proportion of the powders for the composite production was defined from other studies performed with the addition of β-TCP and hydroxyapatite CPCs. Different compositions of the composite 316L stainless steel with hydroxyapatite have been studied in amounts of 0 to 50 wt. % (Silva *et al*., 2013). An example is the study of the hydroxyapatite behavior during the 316L SS sintering, where 5, 10 and 15 wt. % of hydroxyapatite were used to obtain a new composite (Szewczyk-Nykiel and Nykiel, 2010). Another case refers to the development of a biphasic hydroxyapatite/β-TCP cement, with relevant properties as synthetic bone grafts and bioactivity in amounts of 0, 20, 40, 60, 80, and 100 wt. % of β-TCP (Gallinetti *et al*., 2014). The proportions used in this study are shown in Table 1.

Composition	316L SS	β-TCP
1	100 %	0 %
2	95%	5%
3	80%	20%

Table 1
Compositions used in the composites.

After the milling process, the samples were uniaxially pressed with pressure of 619 MPa. In sequence, the samples were sintered in a vacuum furnace up to 1100°C at a 10°C/min rate, maintained for 1 hour and then naturally cooled inside the furnace. The characterization of the composites was performed using a Carl Zeiss EVO® MA15 scanning electron microscope. In the secondary electron mode (SE), the variation of the particles size, the morphology of the forerunner and composites powders were analyzed. In the energy dispersive x-ray mode (EDX), the chemical composition of the composites was evaluated. The samples were also subjected to the compressive resistance test at room temperature to determine their Young's modulus. For the procedure, an Instron® 8001 testing machine with load control condition with an off rate constant cross-head speed of 2 mm/min was used. The results were tested for normality and are shown as the mean ± standard deviation. Differences between groups were evaluated using variance analysis followed by the Student-Newman-Keuls post hoc test. The level of significance was set at $p < 0.05$. The density was evaluated using the Archimedes principle.

3. Results and discussions

Figure 1 shows the forerunner powders of the β-TCP (Figure 1a) and the 316L SS (Figure 1b). As can be seen in Figure 1a, the β-TCP presents particle sizes in a range of 0.5 μm to 5 μm and morphology predominantly irregular, with presence of clusters. In Figure 1b, it is possible to observe that the particle sizes of the 316L SS are localized in a range of 10 μm to 40 μm, also presenting irregular morphology and clusters.

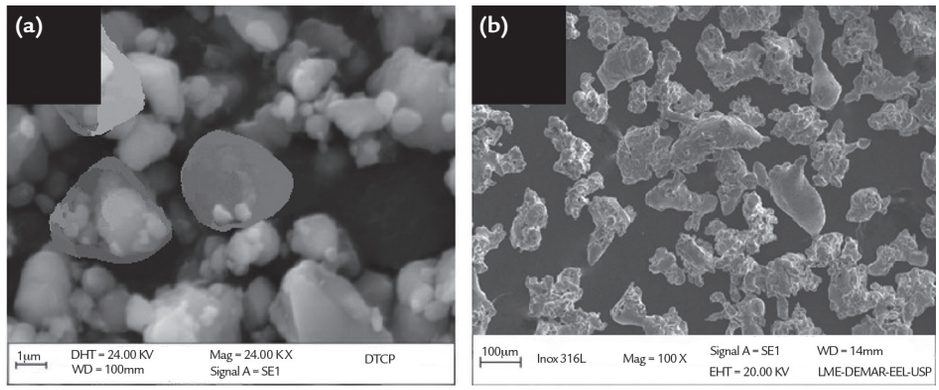

Figure 1
SEM analysis of the forerunner powders (a) β-TCP (b) 316L SS.

The analysis of the compositions 2 and 3 after 10 hours of milling can be seen in Figure 2. In composition 2 (Figure 2a), it is possible to verify that the 316L SS particles presented a flaky morphology with a size smaller than 40 μm. Composition 3 (Figure 2b) showed smaller sizes than composition 2, with particle sizes smaller than 20 μm. The presence of clusters is more pronounced in composition 3.

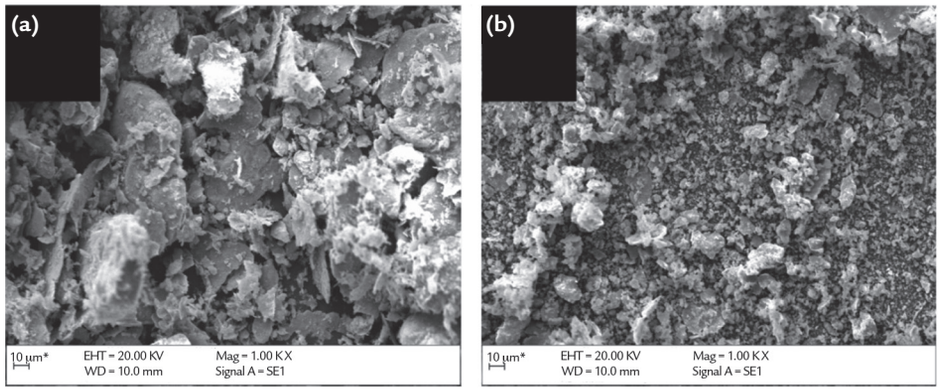

Figure 2
SEM analysis after 10 hours of milling (a) Composition 2 (b) Composition 3.

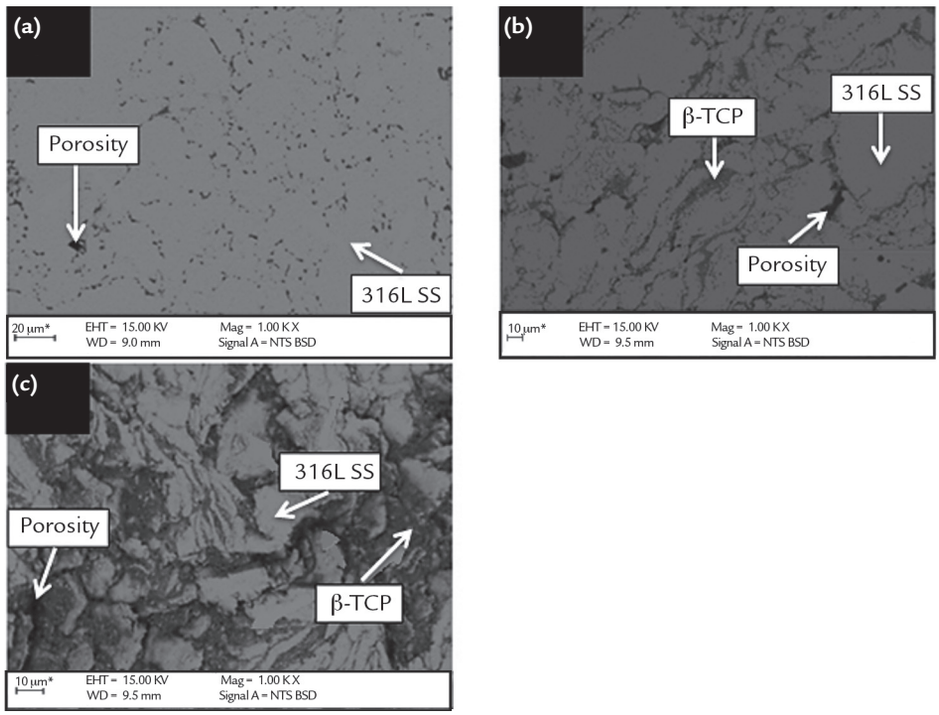

Figure 3
SEM analysis after sintering for (a) Composition 1 (b) Composition 2 (c) Composition 3.

The microstructure of the compositions 1, 2 and 3 sintered at 1100°C can be seen in Figure 3. It is possible to observe in Figure 3a that the pores are not evenly distributed due to the different particle sizes of the 316L SS. In Figures 3b and 3c, corresponding respectively to compositions 2 and 3, it is possible to see that the β-TCP is distributed in the boundary of the 316L SS particles. This is explained through the ductile-brittle alloying mechanism induced during the high energy milling process. During the process, the ceramic particles of the β-TCP become entrapped in the interlamellar spaces of the 316L SS particles due to the high impact between the particles and the milling spheres, which leads the β-TCP particles to show up in the boundary of the 316L SS after sintering (Suryanarayana, 2001).

The Young's modulus obtained through the compressive resistance test for the compositions 1, 2 and 3 is shown in Table 2.

Composition	Young's Modulus (GPa)
1	6.046 ± 0.289
2	2.259 ± 0.032
3	0.863 ± 0.0214

Table 2
Young's modulus of the sintered samples.

It is possible to observe the reduction in the Young's modulus when the amount of β-TCP increases. The β-TCP is a material that has good biodegradability and biocompatibility, but presents low mechanical and fracture resistance after sintering (Tricoteaux *et al.*, 2011; Dong *et al.*, 2002). The value of Young's modulus ranged from 6 GPa for composition 1 (without β-TCP) to 0.82 GPa for composition 3 (with 20% of β-TCP). These values are higher than a porous bone (50 - 400MPa) but smaller than the cortical bone (17 ± 1.7 GPa and 20 ± 1.3 GPa) when measured in the longitudinal direction by mechanical and ultrasonic testing, respectively (Martin *et al.*, 1993; Reilly and Burstein, 1975; Ashman *et al.*, 1984; Zysset *et al.*, 1999).

The low value of Young's modulus obtained for the pure 316L stainless steel (6 GPa) in comparison with the 316L stainless steel obtained through the melting process (200 GPa) is certainly due to the powder metallurgy route, which produces samples with a high percentage of pores. In fact, the metal device that possesses higher elastic modulus than the bone receives most of the load, causing stress shielding in the adjacent bone. The absence of mechanical stimulation with the bone can induce its reabsorption, which may result in failure and loosening of the implant (Navarro *et al.*, 2008; Huiskes *et al.*, 1992; Bauer *et al.*, 1999). Thus, the reduction in the elastic modulus observed by the addition of β-TCP in 316L SS may represent an advantage as regards the shielding tension in the adjacent bone. Another advantage that can be highlighted is the increase of the osteoconductive and osteoinductive properties by adding β-TCP in the 316L SS.

Figure 4 shows the Young's modulus versus the porosity of the compositions 1, 2 and 3. It is possible to note that, by increasing the percentage of β-TCP in the composites, the Young's modulus reduces drastically. It happens due to the increase in the porosity, which reduces the percentage of chemical bonds, and consequently, the mechanical resistance. As can be seen in Figure 4, by adding only 5% of β-TCP to the composite (composition 2), implies in a reduction of 63% in the Young's modulus of this composition. Increasing the percentage of β-TCP to 20% (composition 3), the Young's modulus decreases another 23%. In comparison with the composition 1 without β-TCP addition, it represents a reduction of 86% in the Young's modulus of the composition 3 with 20% of β-TCP (Tricoteaux *et al.*, 2011).

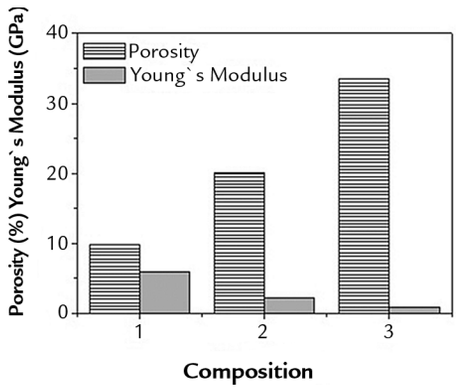

Figure 4
Graph of Young's modulus and porosity of the compositions 1, 2 and 3. The results are presented as the mean ± standard deviation from 3 samples.

The density values obtained after the sintering process can be observed in Figure 5. When comparing the density before sintering (composition 1 = 6.67 g/cm³, composition 2 = 5.40 g/cm³ and composition 3 = 4.07 g/cm³) with the density after sintering (composition 1 = 6.85 g/cm³, composition 2 = 5.99 g/m³ and composition 3 = 4.41 g/cm³), there can be observed an increase of 2.63 % of densification for composition 1, of 9.85 % for composition 2 and 7.71 % for composition 3.

There is a correlation between the decrease in the density values of the sintered samples with the increase of the density in the β-TCP composite. The density obtained for the 316L SS sintered at 1100°C for 1 hour without addition of β-TCP was 85.63 % in comparison with the melted 316L SS (8 g/cm³). With addition of 5% and 20% of β-TCP, these density values decreased to 74.88 % and to 55.13 %, respectively, in comparison with the melted 316L SS. In fact, by increasing the amount of β-TCP in the composites implies a decrease in the density values of the sintered samples. There is a significant statistical difference in the density values of the compositions 2 and 3 when compared with composition 1.

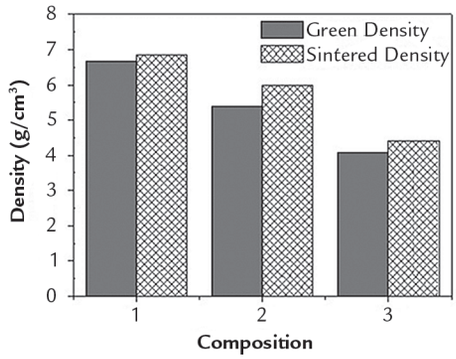

Figure 5
Graph of density of the samples after the sintering process at 1100°C. The results are presented as the mean ± standard deviation from 3 samples. * p< 0.05 when compared with melted 316L SS, sample 1.

The EDX spectrum shown in Figure 6 indicates the quantitative presence of each element that compounds the 316L SS (Fe, Cr and Ni) as well as the β-TCP (Ca and P). As can be seen in Figure 7, the composite has a ratio of 1/3 phosphorus atoms f for each atom of calcium. In fact, this is due to the molecular formula of the β-TCP, where there are 3 atoms of calcium for 1 atom of phosphorus.

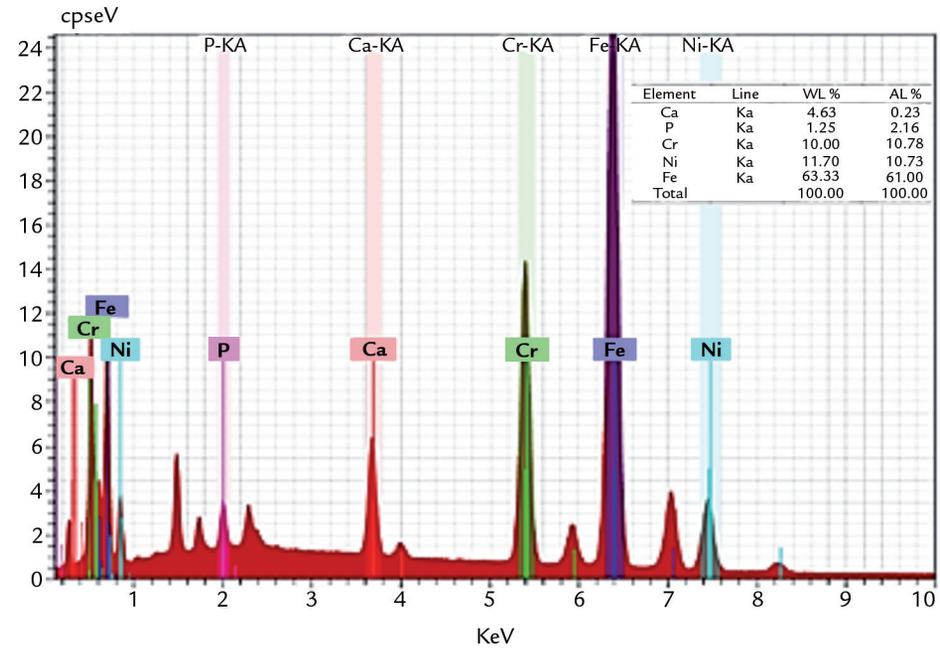

Figure 6
EDX spectra of the composition 2 showing the peaks of Fe, Cr, Ni, Ca, P.

The EDX mapping technique was used to evaluate the distribution of the chemical elements in composition 2 (Figure 7). It is possible to observe the presence of atoms of calcium and phosphorus, which are part of the composition of the β-TCP, as well as the iron, nickel and chromium atoms that correspond to the 316L SS. Clearly seen is a low diffusion of the calcium and phosphorus elements in the matrix of the 316L SS. This could explain the reduction in the compressive strength of the composites by increasing the amount of β-TCP. The elements iron, chromium and nickel occupy the major analyzed region.

Another phenomenon that might have contributed to the reduction in the compressive strength of the composites is observed in Figure 7. By analyzing the

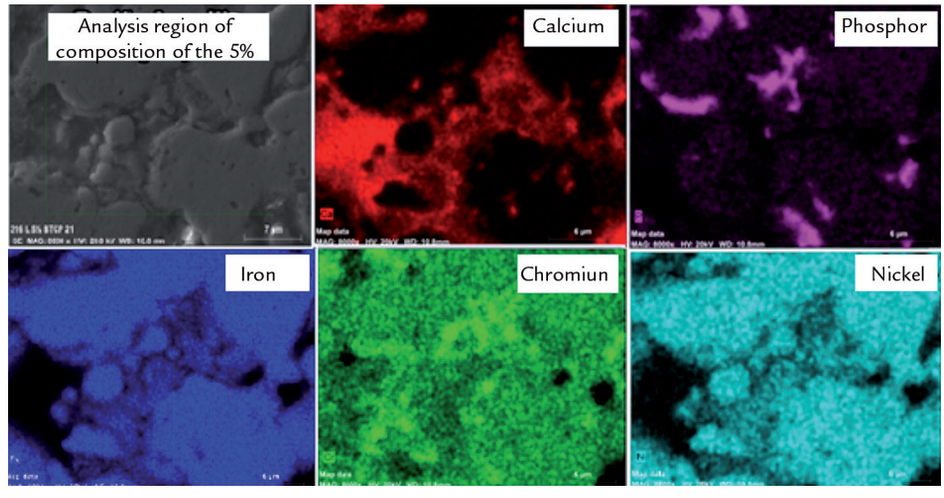

Figure 7
SEM mapping of the atomic composition of the composition 2.

chromium region, it is possible to verify that this chemical element is located cumulatively at the grain boundaries of the sintered sample, which can be explained as sensitization. The sensitization happens very often in austenitic stainless steels as 304L and 316L due to the presence of regions with a low percentage of chromium. It results as a tendency of the chromium to precipitate carbides when subjected to high temperatures and long periods of time, as well as the sintering process (Wang *et al.*, 2016; Doerr *et al.*, 2017). The sensitization can be reversed with the thermal treatment of solubilization and stabilization, which dissolves the chromium carbides from the 316L SS microstructure, remaining only chromium as a solid solution in the austenitic matrix (Gonçalves *et al.*, 2015).

4. Conclusions

The values obtained for the Young's modulus, porosity and density showed that the 316L SS/ β-TCP composites produce by powder metallurgy presented a high percentage of pores in comparison with the melted 316L SS, which is considered the most important parameter to increase the biocompatibility of biomaterials. It was observed that these results are directly related with the increasing of the percentage of β-TCP in the composites, due to the fact that this material has low mechanical resistance.

Acknowledgments

The authors would like to thank the CNPq, CAPES, FAPEMIG and the technicians Jonas Mendes and Marcos Cirilo dos Santos (Universidade Federal de Itajubá, Minas Gerais, Brazil) for their technical assistance.

References

ASHMAN, R. B., COWIN, S. C., BUSKIRK, W. C. V., RICE, J. C. A continuous wave technique for the measurement of the elastic properties of cortical bone. ***Journal of Biomechanics,*** v. 17, p. 349–361, 1984.

ATAOLLAHI O. A., PRAMANIK, S., MEHRALI, M., YAU, Y. H., TARLOCHAN, F., ABU, O. N. A. Mechanical and physical behavior of newly developed functionally graded materials and composites of stainless steel 316L with calcium silicate and hydroxyapatite. ***Journal of the Mechanical Behaviour of Biomedical Materials,*** v. 49, p. 321–31, 2015.

BAUER, T. W., SCHILS, J. The pathology of total joint arthroplasty. II. Mechanisms of implant failure. ***Skeletal Radiology,*** v. 28, p. 483–497, 1999.

BOBBERT, F.S.L., LIETAERT, K., EFTEKHARI, A.A., POURAN, B., AHMADI, S.M., WEINANS, H., ZADPOOR, A.A. Additively manufactured metallic porous biomaterials based on minimal surfaces: a unique combination of topological, mechanical, and mass transport properties. ***Acta Biomaterialia,*** v.53, p. 572–584, 2017.

DOERR, C., KIM, J. Y., SINGH, P., WALL, J. J., JACOBS, L. J. Evaluation of sensitization in stainless steel 304 and 304L using nonlinear rayleigh waves. ***NDT & E International,*** v. 88, p. 17–23, 2017.

DONG, J., UEMURA, T., SHIRASAKI, Y., TATEISHI, T. Promotion of bone formation using highly pure porous β-TCP combined with bone marrow-derived osteoprogenitor cells. ***Biomaterials,*** v. 23, p. 4493–4502, 2002.

GALLINETTI, S., CANAL, C., GINEBRA, M. P. Development and Characterization of biphasic Hydroxyapatite/ β-TCP Cements. ***Journal of the American Ceramic Society,*** v. 97, p. 1065–1073, 2014.

GONÇALVES, R. B., ARAÚJO, P. H. D., BRAGA, F. J. B., TERRONES, L. A. H., PARANHOS, R. P. R. Efeito do tratamento térmico de solubilização e estabilização convencional e alternativo na microestrutura de uma junta soldada com aço inox 347. ***Soldagem & Inspeção,*** v. 20, p. 105–116, 2015.

HUISKES, R., WEINANS, H., RIETBERGEN, B. V. The relationship between stress shielding and bone resorption around total hip stems and the effects of flexible materials. ***Clinical Orthopaedics and Related Research,*** v. 274, p. 124–134, 1992.

JENKO, M., GORENSEK, M., GODEC, M., HODNIK, M., BATI, B. S., DONIK, C., GRANT, J. T., DOLINAR, D. Surface chemistry and microstructure of metallic biomaterials for hip and knee endoprostheses. ***Applied Surface Science,*** v. 427, p. 584-593, 2018.

KAITA, W., HAGIHARA, K., ROCHA, L. A., NAKANO, T. Plastic deformation mechanisms of biomedical Co–Cr–Mo alloy single crystals with hexagonal close-packed structure. ***Scripta Materialia,*** v. 142, p. 111–115, 2018.

KUFFNER, B. H. B., DIOGO, W. S., AMANCIO, D. A., RODRIGUES, G., SILVA,

G. Evaluation of the milling efficiency increase of AISI 52100 steel using niobium carbide addition through high energy ball milling. ***Rem: Revista Escola de Minas,*** v. 68, p. 295-300, 2015.

KUFFNER, B. H. B., SILVA, G., RODRIGUES, C. A., RODRIGUES, G. Study of the AISI 52100 steel reuse through the powder metallurgy route using high energy ball milling. ***Materials Research,*** v.21, n.1, São Carlos 2018, Epub Nov 06, 2017.

LIN, X., YANG, S., LAI, K., YANG, H., WEBSTER, T. J., YANG, L. Orthopedic implant biomaterials with both osteogenic and anti-infection capacities and associated in vivo evaluation methods. ***Nanomedicine: Nanotechnology, Biology, and Medicine,*** v.13, p. 123–142, 2017.

MARTIN, R. B., CHAPMAN, M. W., SHARKEY, N.A., ZISSIMOS, S. L., BAY, B., SHORS, E. C. Bone ingrowth and mechanical properties of coralline hydroxyapatite 1 year after implantation. ***Biomaterials,*** v.14, p.341–348, 1993.

NAVARRO, M., MICHIARDI, A., CASTAÑO, O., PLANELL, J. A. Biomaterials in orthopeadics. ***Journal of the Royal Society Interface,*** v. 27, p. 1137–1158, 2008.

RAO, X., LI, J., FENG, X., CHU, C. Bone-like apatite growth on controllable macroporous titanium scaffolds coated with microporous titânia. ***Journal of the Mechanical Behavior of Biomedical Materials,*** v.77, p.225-233, 2018.

REILLY, D. T., BURSTEIN, A. H. The elastic and ultimate properties of compact bone tissue. ***Journal of Biomechanics,*** v. 8, p. 393–405, 1975.

RICOTEAUX, A., RGUITI, E., CHICOT, D., BOILET, L., DESCAMPS, M., LERICHE, A., LESAGE, J. Influence of porosity on the mechanical properties of microporous β-TCP bioceramics by usual and instrumented Vickers microindentation. ***Journal of the European Ceramic Society,*** v. 31, p.1361–1369, 2011.

SILVA, G., BALDISSERA, M. R., TRICHÊS, E., CARDOSO, K. R. Preparation and characterization of stainless steel 316L/HA composite. ***Materials Research,*** v. 16, p. 304– 309, 2013.

SING, S. L., AN, J., YEONG, W. Y., WIRIA, F. E. Laser and electron-beam powder--bed additive manufacturing of metallic implants: A review on processes, materials and designs. ***Journal of Orthopeadic Research,*** v. 34, p. 369–385, 2016.

SURYANARAYANA, C. Mechanical alloying and milling. ***Progress in Materials Science,*** v. 46, p. 1–184, 2001.

SZEWCZYK-NYKIEL, A., NYKIEL, M. Study of hydroxyapatite behaviour during sintering of 316L. ***Archives of Foundry Engineering,*** v. 10, p. 235–240, 2010.

TORRES, P.M.C., ABRANTES, J.C.C., KAUSHAL, A., PINA, S., DÖBELIN, N., BOHNER, M., FERREIRA, J.M.F. Influence of Mg-doping, calcium pyrophosphate impurities and cooling rate on the allotropic α ↔ β-tricalcium phosphate phase transformations. ***Journal of the European Ceramic Society,*** v. 36, p. 817–827, 2016.

WANG, R., ZHENG, Z., ZHOU, Q., GAO, Y. Effect of surface nanocrystallization on the sensitization and desensitization behavior of Super304H stainless steel. ***Corrosion Science,*** v. 111, p. 728–741, 2016.

ZYSSET, P. K., GUO, X. E., HOFFLER, C. E., MOORE, K. E., GOLDSTEIN, S. A. Elastic modulus and hardness of cortical and trabecular bone lamellae measured by nanoindentation in the human femur. ***Journal of Biomechanics,*** v. 32, p. 1005–1012, 1999.

Received: 4 December 2017 - Accepted: 26 June 2018.